



# Equation of state modeling of the phase equilibria of asymmetric CO<sub>2</sub> + n-alkane binary systems using mixing rules cubic with respect to mole fraction

Martín Cismondi<sup>a,b,c</sup>, Jørgen M. Møllerup<sup>d</sup>, Marcelo S. Zabaloy<sup>a,\*</sup>

<sup>a</sup> Planta Piloto de Ingeniería Química (Universidad Nacional del Sur - CONICET) CC 717, Camino La Carrindanga Km. 7 (8000), Bahía Blanca, Argentina

<sup>b</sup> IDTQ, Facultad de Ciencias Exactas Físicas y Naturales, Universidad Nacional de Córdoba, Av. Velez Sarsfield 1611, Córdoba, Argentina

<sup>c</sup> IVC-SEP, Department of Chemical Engineering, Bygning 229, DTU, DK 2800 Lyngby, Denmark

<sup>d</sup> Prechrom, Christiansholmsvej 26, 2930 Klampenborg, Denmark

## ARTICLE INFO

### Article history:

Received 1 June 2010

Received in revised form 5 October 2010

Accepted 6 October 2010

### Keywords:

Equations of state

Cubic mixing rules

Type III phase behavior

Composition dependence

Critical lines

LLVE

High pressure

Asymmetric systems

Objective function

Interaction parameters

## ABSTRACT

Both the equation of state (EOS) and the quadratic mixing rules proposed by van der Waals towards the end of the XIX century were enormous contributions to the understanding and modeling of fluids phase behavior. They set the basis for a consistent and useful representation of phase equilibria for a great diversity of mixtures. Nevertheless, the models for representing phase equilibria and physico-chemical properties of asymmetric systems may require more flexible mixing rules than the classical quadratic van der Waals (vdW) mixing rules or their equivalent (with regard to the number of available interaction parameters) in modern equations of state.

In particular, the phase equilibria of binary mixtures containing CO<sub>2</sub> and heavy n-alkanes have been studied by an important number of authors and using different types of models, achieving only partially accurate results and realizing the difficulties that these systems showing type III phase behavior (from C14 on) present for predicting or even correlating their phase equilibrium data in wide ranges of temperature and pressure.

Cubic mixing rules (CMRs), implemented as a natural extension of the classical quadratic mixing rules, constitute the simplest alternative among different flexible approaches. In addition, they have the advantage of allowing correlation of multicomponent data by fitting ternary interaction parameters, while leaving invariant the description of the constituent binary systems.

In this work, and after having detected the need for temperature-dependent interaction parameters in a previous study, we implemented an automated parameterization procedure based on characteristic key-points for binary systems showing type III phase behavior. Using the RK-PR EoS coupled to CMRs we present the parameters obtained and results showing for the first time a quite successful complete description of asymmetric CO<sub>2</sub> + n-alkane binary systems, with n-alkane carbon number from 14 to 22.

© 2010 Elsevier B.V. All rights reserved.

## 1. Introduction

Before van der Waals, the liquid state of a substance was believed to be formed of atomic complexes, greater in size than the single molecules existing in the gas phase. Johannes van der Waals expressed "...both portions of the isotherm belong to one curve...there would then only be a difference of greater or smaller density in the two states, and thus only a quantitative difference." [1].

Being such concept, i.e., the continuity between the liquid and vapor states, already a historical contribution, it is remarkable that at the same time van der Waals moved forward and proposed the first model allowing to describe continuously the liquid, vapor and

supercritical states of pure fluids. Today, more than 130 years later, such model continues to be the root of many present equations of state.

*In 1890, Van der Waals provided the practical tools for describing simultaneously both vapor–liquid and liquid–liquid phase separation in binary mixtures, by generalizing his equation of state for application to phase separation of binary fluid mixtures. It was a triumph of the Van der Waals mixture equation that it could produce both vapor–liquid and liquid–liquid phase separation of binary mixtures (Levelt Sengers [2] and ref. cited therein).*

His quadratic mixing rules (QMRs) allowed for a consistent modeling of mixtures phase behavior. Based on the van der Waals EOS and QMRs, van Konynenburg and Scott, "generated the first, nearly comprehensive classification of fluid phase equilibria" [3]. Their calculations were mainly devoted to binary systems without differences in molecular size. They identified five types of fluid phase behavior (I, II, III, IV and V). Studies for size-asymmetric binary sys-

\* Corresponding author. Tel.: +54 291 486 1700; fax: +54 291 486 1600.

E-mail addresses: [mcismondi@efn.uncor.edu](mailto:mcismondi@efn.uncor.edu) (M. Cismondi), [mzabaloy@plapiqui.edu.ar](mailto:mzabaloy@plapiqui.edu.ar) (M.S. Zabaloy).

tems are also available [4]. In combination with later improvements for the density and temperature dependences of the attractive term (including the nowadays classic SRK and PR EOS) the van der Waals approach allowed for a good quantitative representation of vapor–liquid equilibria in a significant number of mixtures studied for decades, including mainly those of interest for the oil and gas or petrochemical industries (see for example [5–7]).

Nevertheless, mixtures which are very asymmetric, either in size or attractive forces, have demonstrated to present a much higher degree of difficulty for their phase behavior modeling. These mixtures appear more frequently in newer applications, including an important diversity of supercritical fluid technologies, such as extraction, fractionation or anti-solvent precipitation, but also in the petroleum industry. One representative and very important family of asymmetric binary mixtures is the CO<sub>2</sub> + n-alkane series. The importance of this series, sometimes taken as a reference in the analysis of other non-alkane + CO<sub>2</sub> binary mixtures, is clear when considering CO<sub>2</sub> injection as a method for enhanced oil recovery or recent approaches for CO<sub>2</sub> sequestration in exploited oil wells.

Available previous attempts to describe the phase equilibria of CO<sub>2</sub> + n-alkane systems in wide ranges of conditions were not completely successful. One of the most interesting and relatively successful approaches has been the one by Polishuk et al. [8]. Using a four-parameter “close-to-cubic” equation of state combined with classical quadratic mixing rules, they proposed generalized equations for the estimation of all repulsive interaction parameters ( $l_{12}$ ) and all temperature-dependent attractive interaction parameters ( $k_{12}$ ) for the whole series of CO<sub>2</sub> + n-alkane binary systems. The constants for their correlation were obtained by considering data only for a few global key-points (KPs). Examples of global key-points are upper critical end points (UCEPs) and local minima or maxima in the pressure–temperature projection of a vapor–liquid critical line. The results of Polishuk et al. [8] showed a good representation of the liquid–vapor part of critical lines while overestimating the size of the liquid–liquid separation region, specially at higher pressures. Predictions for vapor–liquid equilibrium were quite good in general at high temperatures, but overestimation of the CO<sub>2</sub> content in the liquid phase can be observed in the lower temperature region and specially for the heavy liquid under conditions of liquid–liquid–vapor equilibrium (LLVE).

Following a similar approach with the RK-PR EoS [9] and quadratic mixing rules, Cismondi achieved better prediction of critical lines – and also light phase compositions – for CO<sub>2</sub> + n-alkane binary systems, but at the cost of a systematic overestimation of CO<sub>2</sub> solubility in heavy phases [10].

Vitu et al. [11] proposed a group-contribution temperature-dependent functionality for the  $k_{12}$  interaction parameter to be used with the PPR78 EoS [12] and regressed the required constants for some series of binary systems, including CO<sub>2</sub> + n-alkanes. They obtained very good predictions for systems with low or moderate molecular weight for the n-alkane, i.e., those mixtures showing type I or II phase behavior, but predicted type III for CO<sub>2</sub> + n-tridecane (which shows type IV experimentally [13]) and failed to quantitatively describe the behavior of systems showing type III phase behavior (C14 and higher).

Some other works, based on different modeling approaches, achieved only partially successful results, i.e., those studies were restricted to specific types of phase equilibria in relatively narrow ranges of temperature ( $T$ ) and pressure ( $P$ ), instead of considering the global phase behavior of systems in ranges of conditions as wide as those of the available experimental data. For example, Fu et al. [14] show good correlation results using the PC-SAFT EoS for mixtures of CO<sub>2</sub> with light hydrocarbons, and also with heavier n-alkanes, but in this case only for the lower pressure range, without commenting on the very large deviations and systematic overestimation of the phase separation region that occurs at higher

pressures (see also the work by Nguyen-Huynh et al., using a Group-Contribution SAFT equation [15] and ref. cited therein). Recent studies have used excess free energy based mixing rules [16,17], but considering only vapor–liquid equilibria (VLE) in a moderate pressure range, i.e., below 80 bar, for the systems being discussed in this work. The same applies to the use of the recent and more theoretically based PCP-SAFT [18].

Our hypothesis is that such apparent impossibility for a reasonable good description of the complete phase behavior of this type of systems is essentially due to the lack of flexibility, in terms of composition, of the implemented mixing rules.

Cubic mixing rules (CMRs) have been recently proposed as a consistent and natural extension of van der Waals quadratic mixing rules [19]. CMR are the following:

$$a = \sum_{i=1}^N \sum_{j=1}^N \sum_{k=1}^N x_i x_j x_k a_{ijk} \quad (1)$$

$$a_{ijk} = (a_i a_j a_k)^{(1/3)} (1 - k_{ijk}) \quad (2)$$

$$b = \sum_{i=1}^N \sum_{j=1}^N \sum_{k=1}^N x_i x_j x_k b_{ijk} \quad (3)$$

$$b_{ijk} = \left( \frac{b_i + b_j + b_k}{3} \right) (1 - l_{ijk}) \quad (4)$$

where  $N$  is the number of components in a multicomponent mixture,  $a_i$ ,  $b_i$  and  $x_i$  are, for component  $i$ , the attractive energy parameter, the repulsive co-volume parameter and the mole fraction in the system respectively,  $k_{ijk}$  and  $l_{ijk}$  are respectively the energy interaction parameter and the covolume interaction parameter. For a binary system of components 1 and 2, the cubic mixing rules provide four independent interaction parameters, i.e.,  $k_{112}$ ,  $k_{122}$ ,  $l_{112}$  and  $l_{122}$ . Thus, the number of available interaction parameters in cubic mixing rules doubles the number which quadratic mixing rules provide. The conventional quadratic mixing rules are a particular case of cubic mixing rules [19]. Recently, Polishuk has used CMRs but in a form that cannot be extended to multicomponent mixtures [20].

For ternary or higher systems, Eqs. (2) and (4) require ternary interaction parameters. Such parameters can be either regressed from experimental information on ternary systems or predicted from parameters obtained from experimental data on binary systems [19]. The potential correlation of ternary data by fitting ternary interaction parameters, while leaving invariant the description of the constituent binary systems, makes the CMR very appealing and some promising preliminary results have been presented by Pisoni et al. [21]. The partial molar properties for component 1, when component 1 is infinitely diluted in component 2, depend on  $k_{122}$  and on  $l_{122}$  but not on  $k_{112}$  and  $l_{112}$ . Analogously, the partial molar properties for component 2, when component 2 is infinitely diluted in component 1, depend on  $k_{112}$  and  $l_{112}$  but not on  $k_{122}$  and  $l_{122}$  [19]. Thus, the dominant interaction parameters for a given concentration limit are clearly identified for CMRs.

Our general goal is to explore and analyze the possibilities that these flexible, yet simple, cubic mixing rules offer for modeling the high pressure phase behavior of different types of asymmetric mixtures, identifying their strengths and limitations. In previous preliminary works [22,23], we used CMRs in combination with the RK-PR EoS [9] and focused on the binary carbon dioxide (1) + n-hexadecane (2), as a representative case of the most common phase behavior observed for asymmetric systems of interest, known as type III in the classification of Scott and van Konynenburg [24]. In the first work we carried out a parameter sensitivity analysis that paid attention to the global phase equi-

librium behavior using the GPEC software [25,26] and arrived to a unique set of (temperature-independent) cubic interaction parameters, which showed a clear improvement over the performance of quadratic mixing rules for CO<sub>2</sub> (1) + n-hexadecane (2) [22]. Nevertheless, the results suggested that a proper description of the phase equilibria for this system would require the introduction of temperature dependent interaction parameters. We did so later, proposing a consistent temperature dependence for the  $k_{112}$  and  $k_{122}$  parameters. The results demonstrated that, in combination with temperature dependent attractive interaction parameters, the flexibility that cubic mixing rules offer in composition, in comparison to the classical quadratic mixing rules, can be used to quite accurately represent the phase equilibria of very asymmetric mixtures [23].

The present work deals with the procedure and results for the automated numerical optimization of the interaction parameters of CMRs coupled to the RK-PR EOS for reproducing the fluid phase behavior for all the CO<sub>2</sub> + n-alkane binary mixtures experimentally showing type III phase behavior, i.e., those with n-alkane carbon numbers from 14 to 22. Our final goal is to improve the description of the phase equilibria of such systems with respect to previous approaches and to verify our previously stated hypothesis.

## 2. Methodology

Our goal is clearly to optimize the representation of the fluid phase behavior over a wide range of conditions for the CO<sub>2</sub> + n-alkane binary mixtures with n-alkane carbon number from 14 to 22, using cubic mixing rules (CMRs) with temperature dependent attractive interaction parameters.

When translating a general objective like that into specific tasks to be performed, a number of choices have to be made with regard to, e.g., the particular equation of state, the pure compound parameters, the experimental data sets to be considered, the definition of the objective function, etc.

In the following sections, we discuss some details and comment on each of these issues, which define as a whole the methodology we followed in the study presented in this work.

### 2.1. Equation of state

CMRs can be used, in principle, with any equation of state susceptible of implementation of one-fluid type mixing rules. We believe that, roughly, the ability of an equation-of-state (EoS) type model to represent the phase behavior of real mixtures, with regard to the relationship among  $T$ ,  $P$  and phase compositions, depends more on the mixing rules used than on the form of the relationship among temperature, pressure and molar volume for the pure compounds, provided that the EOS properly reproduces the experimental pure compound liquid–vapor saturation line. Therefore, considering the relative simplicity of van der Waal's type cubic equations of state, and that they continue to be the most used models for representing phase equilibrium, specially for practical applications, we decided to use CMRs in combination with cubic equations of state (CEOS). CEOS, never give more than three real molar volume roots at a given temperature (as long as the mixing rules are not density-dependent). Other more modern EOSs may lead to inconsistent behavior due to the appearance of more than three roots, at set temperature, for a given pure compound. For instance, Privat et al. [27] have recently shown, very clearly for pure n-decane (see their Fig. 12), that the PC-SAFT EOS gives three stable fluid–fluid saturation curves that meet at a triple pure-compound liquid–liquid–vapor point. Multiple stable fluid–fluid saturation lines and stable fluid–fluid–fluid triple points have never

**Table 1**

Pure compound parameters<sup>a</sup> for the RK-PR EOS (this work).

Compound	$a_c$ (bar $\times$ L <sup>2</sup> /mol <sup>2</sup> )	$b$ (L/mol)	$\delta_1$	$k$
Carbon dioxide	3.8796	0.027595	1.995049	2.14904
n-Tetradecane	106.1728	0.241220	4.483807	2.95470
n-Pentadecane	118.3736	0.257929	4.659300	3.04467
n-Hexadecane	131.2301	0.275390	4.804542	3.10300
n-Heptadecane	141.9859	0.293282	4.787073	3.26364
n-Octadecane	155.2174	0.310493	4.939278	3.34726
n-Nonadecane	168.3692	0.328251	5.038376	3.43935
n-Eicosane	180.7048	0.345322	5.100415	3.57697
n-Heneicosane	194.4869	0.362952	5.197945	3.64879
n-Docosane	209.6567	0.379792	5.365185	3.68889

<sup>a</sup> They reproduce the experimental (DIPPR, [31])  $T_c$ ,  $P_c$ , acentric factor and liquid molar volume at triple point.

been found experimentally for pure compounds, according to current knowledge.

The results from preliminary studies for the representation of experimental ternary mixtures phase diagrams with CMRs did not show important differences between using the Peng–Robinson or the RK-PR equation of state [21].

In this work, due to its better representation of volumetric properties, we used the three-parameter RK-PR EoS [9]:

$$P = \frac{RT}{v-b} - \frac{a}{(v+\delta_1 b)(v+(1-\delta_1/1+\delta_1)b)}; \quad (5)$$

$$a_i(T) = a_{c,i} \left( \frac{3}{2 + T/T_{c,i}} \right)^{k_i}$$

(with linear mixing rule for the third parameter  $\delta_1$ ) which in contrary to the limitations of the SRK or PR equations should lead to a good prediction of densities when correlating phase equilibrium in the pressure–temperature–composition ( $P$ – $T$ – $z$ ) space. Besides, the RK-PR EoS has been found to provide a better correlation capacity for synthetic natural gas mixtures when compared to other EoS like PR and even PC-SAFT (consider results in ref. [28,29]). Recently, the RK-PR model was also successfully used for the dynamic modeling of a liquefied gas tank in wide ranges of temperature and pressure, with internal energy, volume and numbers of moles as independent thermodynamic variables [30].

### 2.2. Pure compound parameters

Having one extra parameter in comparison to classical cubic EoS's like SRK and PR, the RK-PR model allows to match the critical temperature ( $T_c$ ) and critical pressure ( $P_c$ ), and also the acentric factor for a given pure compound, while leaving one degree of freedom for the adjustment of volumetric properties. In the original paper, a universal value of 1.168 for the ratio between calculated and experimental critical compressibility factors ( $Z_c$ ) was proposed as a default specification when no other information is available [9]. In this work, instead, we decided to match the experimental liquid molar volume at the triple point for each compound. The values were taken from the DIPPR database [31] and the resulting parameters are presented in Table 1.

### 2.3. The temperature dependence for the $k_{112}$ and $k_{122}$ parameters

In our previous preliminary studies [22,23] we found that a temperature dependence was needed for the attractive interaction parameters, i.e., for  $k_{112}$  and  $k_{122}$ , in binary systems, and defined the following functionality, which has finite limits both at zero and

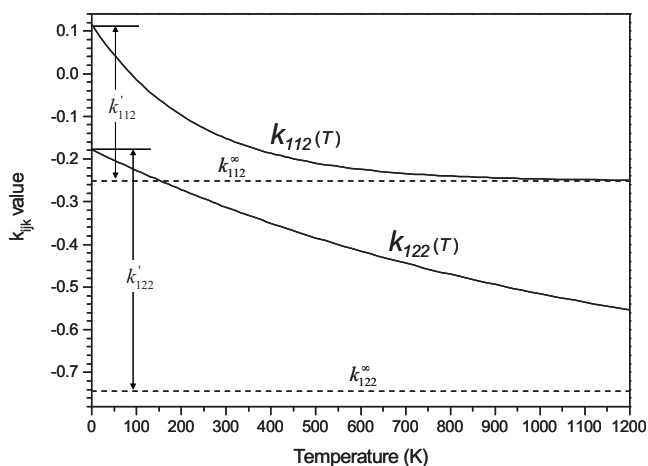


Fig. 1. The behavior of  $k_{112}$  and  $k_{122}$  for the system  $\text{CO}_2$  (1) + n-hexadecane (2) as a function of temperature, according to Eq. (6) and parameters in Table 5.

at infinite temperature.

$$k_{ijk} = k_{ijk}^{\infty} + k'_{ijk} e^{-T/T_{ijk}^*} \quad (6)$$

It can be seen that this is a monotonically decreasing or increasing function of temperature, depending on the sign of  $k'_{ijk}$ . Parameter  $k_{ijk}$  asymptotically tends to  $k_{ijk}^{\infty}$  [Eq. (6)]. Fig. 1 shows how  $k_{112}$  and  $k_{122}$  depend on temperature for the case of  $\text{CO}_2$  (1) + n-hexadecane (2) according to parameters obtained in this work. In Section 3 we show the curves for all systems considered, in a restricted temperature range of interest.

#### 2.4. Definition of key-points and other data

When fitting parameters to obtain a good correlation of experimental phase equilibria it is common practice to include a large number of data points in the objective function, usually all points available. In this work we followed a different approach for a number of reasons.

First of all, it is a fact that there is a considerable scatter in the data available for asymmetric systems like  $\text{CO}_2$  + heavy n-alkane, specially for the compositions of two phases at equilibrium. There can be different reasons for this and they will be explored and discussed in a subsequent publication.

Second, van der Waals type equations of state provide qualitatively correct patterns for phase diagrams and their evolution, and some regions are much sensitive to interaction parameters than others. Taking that into account, it was found that it is possible to achieve a good parameterization for describing the global phase behavior of a system by considering only a few carefully selected key-points (KPs), instead of the indiscriminated totality of points available. This was shown by Polishuk et al. (see for example [8,32] for the series of  $\text{CO}_2$  binary mixtures with alkanols and n-alkanes) and then by Cismondi (types II and III for  $\text{CO}_2$  + n-alkane binary systems [10]) and Secuianu et al. ( $\text{CO}_2$  + alkanol binary systems showing type I or II [33–35]).<sup>1</sup>

Finally, we are not interested just in correlating some particular isotherms or isobars for a limited number of systems. Our goal is to describe the global phase behavior, in wide ranges of  $T$  and  $P$ , and paying attention to the evolution of such behavior in nine differ-

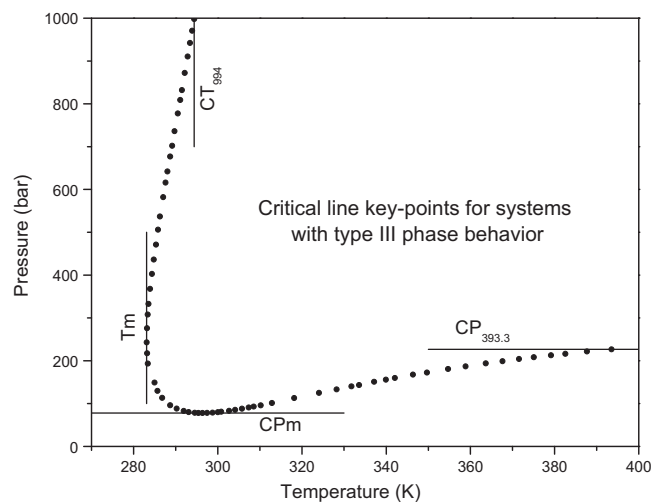


Fig. 2. Illustration of the four key-points defined for the representation of a critical line, for the case  $\text{CO}_2$  (1) + n-tetradecane (2). See Table 2 for numerical values.

ent consecutive binary systems of the  $\text{CO}_2$  + n-alkane homologous series. Therefore, we would prefer, or even need, a single procedure and a single objective function form, both valid and equivalent for all systems considered.

In this work, having an important degree of model flexibility provided by the CMRs, we decided to consider a sufficient number of key-points for properly placing both the critical line and the liquid branches of the LLV line of each system.

Each critical line is represented by four particular key-points, defined previously by Cismondi [10] for systems with type III phase behavior. They are illustrated in Fig. 2 for the case of  $\text{CO}_2$  + n-tetradecane: Cpm is pressure coordinate of the local minimum of the curve;  $T_m$  the minimum temperature in the liquid–liquid like part of the critical line.  $CT_{994}$  represents the critical temperature at the maximum pressure experimentally available for these lines and, accordingly,  $CP_{393.3}$  represents the critical pressure at the maximum temperature experimentally available. More details are given in Table 2, which reports the critical line key-point values for all systems considered. Those for systems with n-alkane carbon numbers 14 to 17, 19 and 22 were taken from the critical lines measured in Bochum, Germany, by the Group of Prof. Schneider [36,37]. These data show a consistent and smooth evolution from one system to another along the series. For that reason, we generated the corresponding key-points for C18, C20 and C21 by predicting values from a regression for the whole series (values with superscript a in Table 2).

For representing the LLV behavior of each binary system we defined six key-points which provide information regarding the low temperature and middle temperature ranges, besides the Upper Critical End Point (UCEP) which marks the maximum temperature limit of the three-phase line. More details are given in Table 3, which reports the values for the six key-points considering the nine binaries from C14 to C22. Table 3 also informs the values assigned to  $T_{lowLLV}$  and  $T_{midLLV}$  which are somewhat arbitrary, depending on the experimental data available for each system.

We found no LLV data for the binaries with C17, C18 and C22. Analogous to what we did for critical line key-points, we generated artificial LLV key-points for these three systems based on the observation of the data for the whole series. Fig. 3 shows both the experimental and generated key-points for all the binaries considered, from C14 to C20. Notice that, although we use some generated key-points in our parameter fitting procedure, we assess the quantitative performance of the final parameter values through comparisons only with experimental data.

<sup>1</sup> The success in all those works was limited, as already pointed out in Section 1. But the main reasons for that were found not in the approach based on key-points, but in the limitations of quadratic mixing rules. That is our conclusion, supported now by the results achieved in the present work.



**Table 2**

Critical line key-points considered in this work for CO<sub>2</sub> + n-alkane binary mixtures. CN: carbon number of the n-alkane. Temperatures are expressed in K and pressures in bar. CT<sub>994</sub>: critical temperature assigned to a pressure value of 994 bar. The pressures informed in the references range from 991 to 997.8 bar. CP<sub>393.3</sub>: critical pressure assigned to a temperature value of 393.3 K. The temperatures informed in the references range from 393.14 to 393.59 K.

CN	CT <sub>994</sub> (K)	T <sub>m</sub> (K)	CP <sub>m</sub> (bar)	CP <sub>393.3</sub> (bar)	References for experimental data (values)
14	294.40	283.1	78	226.6	Scheidgen [37]
15	299.54	290.0	121	237.8	Scheidgen [36] Scheidgen and Schneider [47]
16	305.45	297.6	166	256	Scheidgen [36] Spee and Schneider [48]
17	311.43	304.7	203	272.2	Scheidgen [37]
18	316.4 <sup>a</sup>	311.0 <sup>a</sup>	237.9 <sup>a</sup>	287	Pöhler [42]
19	321.51	317.2	269	304	Scheidgen [37]
20	326.5 <sup>a</sup>	323.2 <sup>a</sup>	299.8 <sup>a</sup>	320	Kordikowski and Schneider [43]
21	331.3 <sup>a</sup>	328.9 <sup>a</sup>	326.2 <sup>a</sup>	338.6 <sup>a</sup>	
22	335.97	334.2	350	357	Scheidgen [37]

<sup>a</sup> Values obtained from regressions based on experimental data for other CN.

**Table 3**

Liquid–liquid–vapor equilibrium (LLV) key-points considered in this work for CO<sub>2</sub> + n-alkane binary mixtures. Six LLV key-points are considered: composition of the two liquid phases at a selected low temperature T<sub>lowLLV</sub> (x<sub>lowLLV</sub> and y<sub>lowLLV</sub>). Composition of the two liquid phases at a selected mid-range temperature T<sub>midLLV</sub> (x<sub>midLLV</sub> and y<sub>midLLV</sub>). Temperature and composition of the alkane-richer phase at the upper critical end point (T<sub>UCEP</sub> and x<sub>UCEP</sub>). CN: carbon number of the n-alkane. Temperatures are expressed in K. x and y: CO<sub>2</sub> molar fraction.

CN	T <sub>lowLLV</sub> (K)	x <sub>lowLLV</sub>	y <sub>lowLLV</sub>	T <sub>midLLV</sub> (K)	x <sub>midLLV</sub>	y <sub>midLLV</sub>	T <sub>UCEP</sub> (K)	x <sub>UCEP</sub>	References for experimental data
14	270.0	0.707	0.9815	291.2	0.819	0.9631	311.2	0.820 <sup>a</sup>	van der Steen et al. [38] and Hottovy et al. [39]
15	273.4	0.689	0.9847	293.5	0.767	0.9785	309.4	0.769 <sup>a</sup>	van der Steen et al. [38] and Hottovy et al. [39]
16	283.2	0.716	0.9868	298.1	0.751	0.9898	307.9 <sup>b</sup>	0.749 <sup>a</sup>	van der Steen et al. [38]
17	287.0 <sup>c</sup>	0.712 <sup>c</sup>	0.9900 <sup>c</sup>	298.0 <sup>c</sup>	0.736 <sup>c</sup>	0.9925 <sup>c</sup>	306.8 <sup>b</sup>	0.740 <sup>b</sup>	
18	290.0 <sup>c</sup>	0.708 <sup>c</sup>	0.9930 <sup>c</sup>	298.0 <sup>c</sup>	0.725 <sup>c</sup>	0.9947 <sup>c</sup>	306.0 <sup>b</sup>	0.729 <sup>b</sup>	
19	292.9	0.704	0.9958	298.5	0.716	0.9966	305.5	0.722 <sup>a</sup>	Fall et al. [40]
20	300.3	0.716	0.9985	302.5	0.715	0.9985	305.2	0.714 <sup>a</sup>	Fall et al. [40]
21	301.5	0.708	0.9986	303.4	0.710	0.9986	305.0	0.709 <sup>a</sup>	Fall et al. [40]
22	301.0 <sup>c</sup>	0.702 <sup>c</sup>	0.9987 <sup>c</sup>	303.0 <sup>c</sup>	0.706 <sup>c</sup>	0.9987 <sup>c</sup>	304.8 <sup>b</sup>	0.706 <sup>b</sup>	

<sup>a</sup> Values for x<sub>UCEP</sub> estimated from LLV data at temperatures below the UCEP.

<sup>b</sup> Values obtained from regressions based on UCEP experimental data and pseudo-experimental data for other CN.

<sup>c</sup> Artificial LLV points estimated based on data for other CN (see Fig. 3).

LLV data for the binaries with C14, C15 and C16 were taken mainly from van der Steen et al. [38]. Hottovy et al. [39] had also reported data for the binaries with C14 and C15 but these data may present larger uncertainties (probably due to assuming the vapor phase as pure carbon dioxide, see van der Steen et al. [38]).

Note that the binary with n-docosane does not show LLVE experimentally (Table 3), due to the precipitation of solid n-docosane [40]. Artificial LLVE data were also generated for this binary, in order to follow the same procedure applied to lighter n-alkanes for the parameterization of their interactions with CO<sub>2</sub> for the representation of fluid phase equilibrium.

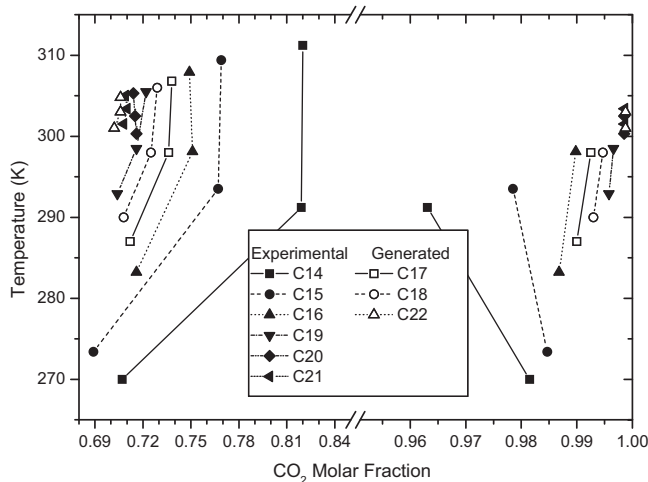


**Fig. 3.** Experimental and generated LLV key-points (composition of the liquid phases) selected for their use in the objective function (see Table 3) corresponding to CO<sub>2</sub> + n-alkane systems.

Besides the critical line and LLV key-points considered for all systems, we also evaluated the possibility of adding experimental two-phase equilibrium compositions at specified temperature and pressure to the database used to fit the model parameters. After trying also with some points for C19 and C20, in the final results shown in Section 3 only the data specified in Table 4 for CO<sub>2</sub> (1) + n-hexadecane (2) were considered. Note that the points taken from Brunner et al. [41] at 573 K allowed us to considerably extend the temperature range covered.

There are also unpublished Pxy and Txy data in the PhD thesis by Pöhler [42], which Prof. Schneider kindly provided us with, together with the already cited thesis by Scheidgen [37]. The data by Pöhler concerns the binary systems of CO<sub>2</sub> with C17, C18 and C22. Nevertheless, and taking for example the data at 393.2 K, they do not follow a trend when put together with the data for C16 in Table 4 and other published data for C19 and C20 from the same group in Bochum [43], and not even among themselves. For this reason, we used only critical lines data from the thesis by Scheidgen (which do show regular trends, as already pointed out, see Table 2) but no compositional data for phase separation was taken from these thesis for use in the objective function.

**Table 4**

Two-phase experimental equilibrium points considered in the objective function for the parameterization of CO<sub>2</sub> (1) + n-hexadecane (2) binary mixture. x<sub>1</sub> and y<sub>1</sub> are mole fractions of CO<sub>2</sub> in the heavy and light phase respectively.

T (K)	P (bar)	x <sub>1</sub>	y <sub>1</sub>	Reference
393.2	100	0.4968	0.9982	Spee and Schneider [48]
393.2	200	0.7473	0.9909	Spee and Schneider [48]
573.2	101	0.428	0.962	Brunner et al. [41]
573.2	201	0.700	0.938	Brunner et al. [41]

**Table 5**  
Optimum CMR parameters obtained, with the corresponding minimum value found for the objective function (OF). Eq. (6) was used with  $T_{112}^* = 230$  K and  $T_{122}^* = 1100$  K in all cases. CN: carbon number of the alkane in the binary system CO<sub>2</sub> (1) + n-alkane (2).

CN	$k'_{112}$	$k'_{122}$	$k^{\infty}_{112}$	$k^{\infty}_{122}$	$l_{112}$	$l_{122}$	Terms	OF
14	0.39714	0.55412	-0.24429	-0.70425	0.05028	0.02446	15	0.01041
15	0.38194	0.56133	-0.24851	-0.72217	0.05918	0.03310	15	0.00550
16	0.36666	0.56603	-0.25117	-0.74370	0.07140	0.04106	31	0.00995
17	0.48983	0.57027	-0.32618	-0.81594	0.06434	0.06220	15	0.00009
18	0.43254	0.56899	-0.30442	-0.82480	0.06682	0.03727	15	0.00007
19	0.48211	0.69346	-0.32164	-0.94012	0.07207	0.02923	15	0.00007
20	0.29759	0.10168	-0.31339	-0.54799	0.06345	0.05074	15	0.00015
21	0.19131	0.38747	-0.25494	-0.74192	0.06374	-0.01493	15	0.00014
22	0.11505	0.24985	-0.24667	-0.65598	0.06365	-0.01199	15	0.00021

## 2.5. Objective function and optimization

Having already defined our key-points, now we need to specify how they will be mathematically introduced in the objective function. For temperature and pressure values such as those of Table 2, in order to neutralize the arbitrary choice of units and trying to avoid weight factors, we decided to use the square of the relative deviation for the corresponding term in the objective function, which is a natural choice and common practice in defining objective functions.

At the beginning we did the same (relative differences) for composition key-points, such as those in the third and fourth column of Table 3, using CO<sub>2</sub> mole fractions, but soon realized that each compositional point should count for two, considering terms for both compound 1 and compound 2 (the alkane in this case) in order to give also a reasonable weight to phases rich in CO<sub>2</sub>. Moreover, for composition points we have observed that using squares of relative deviations gave too much weight to those terms accounting for deviations in the n-alkane mole fraction when it is of the order or around  $10^{-3}$  or smaller, in detriment of the representation of the other points, specially the critical line. On the other hand, if we define objective function terms as the square of the absolute difference between the calculated and experimental mole fractions, then we do not penalize properly the objective function for the cases of important relative errors in CO<sub>2</sub> rich phases. We finally found that using the square of the absolute difference divided by the experimental value led to a proper balance in the objective function and allowed us to achieve the results presented in this work.

Therefore, the objective function (OF) takes the following form:

$$OF = \sum_{i=1}^5 \left( \frac{KP_i^{calc} - KP_i^{exp}}{KP_i^{exp}} \right)^2 + \sum_{j=1}^{Nz} \left[ \frac{(z_{j,1}^{calc} - z_{j,1}^{exp})^2}{z_{j,1}^{exp}} + \frac{(z_{j,2}^{calc} - z_{j,2}^{exp})^2}{z_{j,2}^{exp}} \right] \quad (7)$$

where  $KP_i$  is a temperature or pressure key-point [there are four critical key points (Table 2) plus a  $T_{UCEP}$  key point (Table 3)] and the mole fractions  $z_{j,1}$  and  $z_{j,2}$  correspond to a compositional key-point in Table 3 or to two-phase equilibrium compositions (Table 4) when they are used. For a given binary CO<sub>2</sub> + n-alkane system, the total number of compositional points  $Nz$  will then be five (from Table 3) plus the number of phase compositions to be considered from specific two-phase points.

To fix ideas, note that the objective function for each system using only the key-points given in Tables 2 and 3 will contain 15 terms (since a given compositional key point of Table 3 contributes with two terms to the objective function OF), while two extra terms will be added per each phase composition of two-phase equilibrium points (eight phases, contributing with 16 terms, when considering

Table 4 for C16, leading to a total count of 31 terms in the objective function OF).

## 2.6. Phase equilibrium calculations

All calculated values required by the objective function were obtained using a reduced and adapted GPEC algorithm [25]. The numerical continuation methods used to generate the different lines involved and the set of equations for each specific type of calculation are described elsewhere [44–46]. Predicted global key-points (see Section 2.4 and Tables 2 and 3) were detected while following the calculation of the main critical line and the LLV line according to the general scheme illustrated by Fig. 1 in [45]. Biphasic calculations for single  $T$ ,  $P$  specifications (see Table 4) were performed solving the following reduced set of equations like described in [44]:

$$X = \begin{bmatrix} \ln x_1 \\ \ln y_2 \\ \ln v_x \\ \ln v_y \end{bmatrix}; \quad F = \begin{bmatrix} \ln P_x(x, T, v_x) - \ln P \\ \ln P_y(y, T, v_y) - \ln P \\ \ln \hat{f}_1^x(x, T, v_x) - \ln \hat{f}_1^y(y, T, v_y) \\ \ln \hat{f}_2^x(x, T, v_x) - \ln \hat{f}_2^y(y, T, v_y) \end{bmatrix} = 0 \quad (8)$$

where  $X$  is the vector of independent variables and  $F=0$  is the set of equations to solve. Experimental values were used as initial estimates for the phase mole fractions ( $x$  and  $y$ ) and initial  $v_x$  and  $v_y$  molar volume values were obtained by solving the pressure equation at the specified  $T$  and  $P$ . The system of Eq. (8) accounts for the uniformity of temperature, pressure and component fugacities throughout the two phase system under equilibrium conditions.

Phase diagrams shown in Section 3 were also generated with GPEC [26]. Pxy and Txy diagrams are organized in regions, which are calculated after identifying the limiting points of such regions, as a number of intersections between a straight line corresponding to the specified temperature or pressure [44] and the

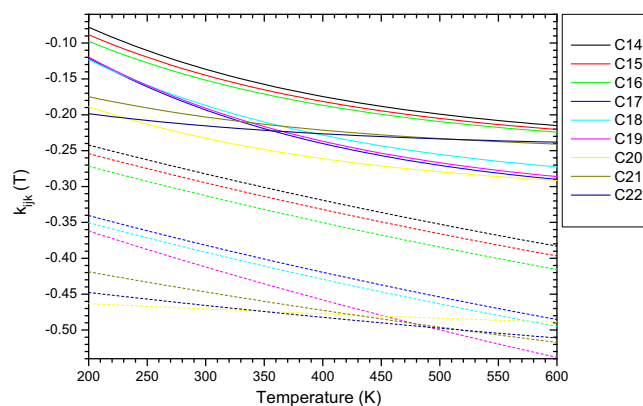


**Fig. 4.** Behavior of the interaction parameters  $k_{112}$  (solid lines) and  $k_{122}$  (dashed lines) as a function of temperature, according to Eq. (6) and Table 5, for the nine CO<sub>2</sub> (1) + n-alkane (2) systems studied.

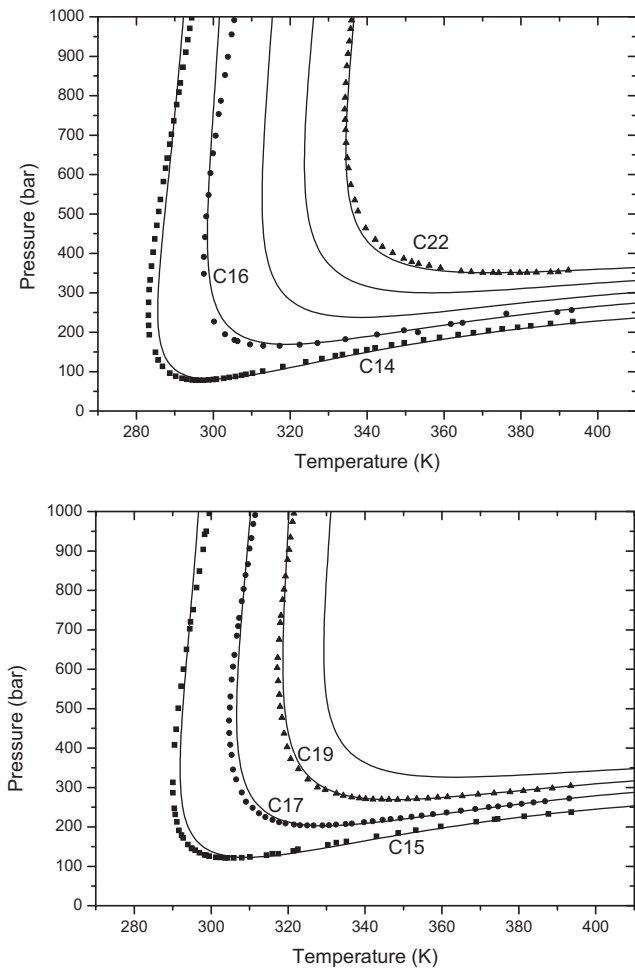


**Fig. 5.** Critical lines for  $\text{CO}_2$  + n-alkane binary systems with type III phase behavior. Even and odd carbon number systems in the upper and bottom part respectively. References for data points are given in Table 2. Lines were calculated with the RK-PR EOS coupled with CMRs and parameters from Tables 1 and 5.

univariant lines of the global phase equilibrium diagram (i.e., LLV, critical, azeotropic or pure-compound vapor–liquid lines in the pressure–temperature space).

### 3. Results

We first conducted minimizations for the system  $\text{CO}_2$  (1) + n-hexadecane (2) using different initial sets of parameters, and leaving free either six or eight parameters. In the first case,  $T_{112}^*$  and  $T_{122}^*$  were kept at constant values. We found that  $T_{112}^* = 230\text{ K}$  and  $T_{122}^* = 1100\text{ K}$  led to the minimum value for the objective function OF, which was – as expected – more influenced by the other six constants for each system:  $l_{112}$ ,  $l_{122}$ ,  $k'_{112}$ ,  $k'_{122}$ ,  $k^{\infty}_{112}$  and  $k^{\infty}_{122}$ . We therefore decided to keep those constant  $T^*$  values for all the systems and proceeded to the minimization with six parameters in each case.

Table 5 shows the final interaction parameter sets for the nine systems studied, with the n-alkane varying from C14 to C22. These are the CMR parameters that, using the RK-PR EoS with pure compound parameters from Table 1, gave in each case the minimum value for the objective function OF defined in Section 2.5. The relatively high value in the objective function OF for C16, when compared to the other systems, is naturally explained by the extra terms involving the data in Table 4, which are not present for the rest. On the contrary, the higher values for C15 and specially C14 might be explained by more extreme shapes of the highly non-

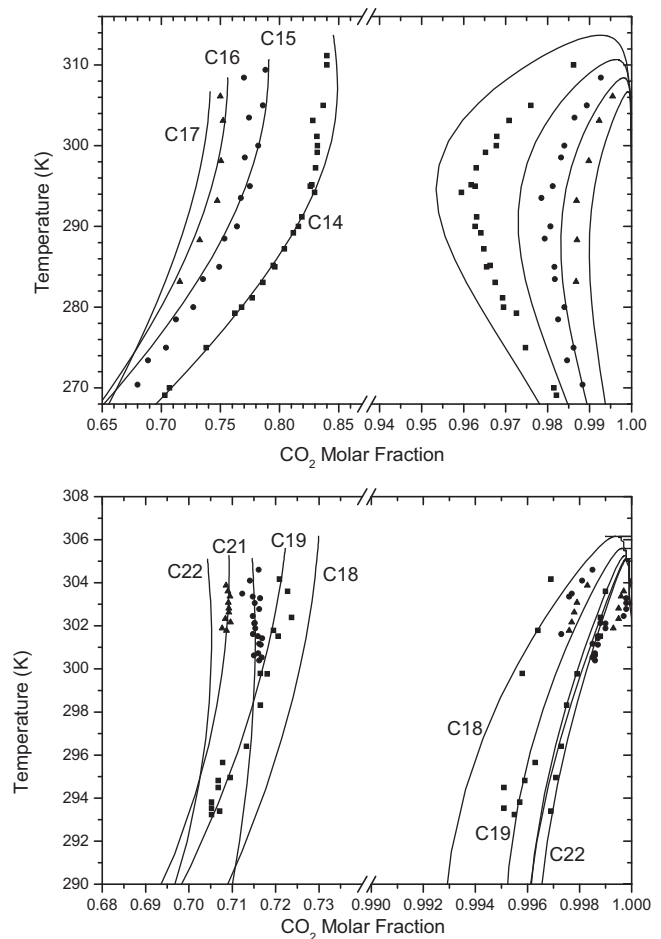


**Fig. 6.** Branches of the LLV equilibrium lines for  $\text{CO}_2$  + n-alkane binary systems with type III phase behavior. Data points taken from van der Steen et al. [38] (C14–C15–C16), Hottovy et al. [39] (C14–C15) and Fall et al. [40] (C19–C20–C21). Lines were calculated with the RK-PR EOS coupled with CMRs and parameters from Tables 1 and 5.

linear critical lines (and very low CPM), related to the proximity to type IV phase behavior, which is observed for C13 with  $\text{CO}_2$ .

Note that all  $k'$  values are positive, which means that all  $k$  functions decrease with temperature, as it can be observed in Fig. 4. Also notice that all  $k^{\infty}$  are negative, while the repulsive interaction parameters ( $l_{112}$  and  $l_{122}$ ) fall all in the range from  $-0.015$  to  $0.072$ . Moreover, some regular trends can be observed, specially among the first three systems.

Figs. 5 and 6 show the evolution of the global phase behavior along the series through calculated critical lines in the  $P$ – $T$  space (Fig. 5) and through computed phase compositions along LLV lines in the temperature–composition space (Fig. 6). Note the high quality of the critical lines description both in the vapor–liquid and in the liquid–liquid regions, equivalent to or better than in previous attempts (see references in Section 1) but achieving simultaneously a good description of the composition of heavy phases under LLV conditions. The same is observed in Fig. 7, where Pxy diagrams of  $\text{CO}_2$  + n-hexadecane are presented for different temperatures ranging from 313.2 to 573.2 K. Also in Fig. 8, with Txy diagrams for the same system and pressures between 100 and 250 bar, we see a good performance. The high correlation capability offered by the CMRs flexibility is therefore demonstrated through these modeling results for  $\text{CO}_2$  + n-hexadecane, which may then be regarded as semi-predictive, since only a few but sufficient, consistent and carefully selected, experimental data points, covering wide ranges

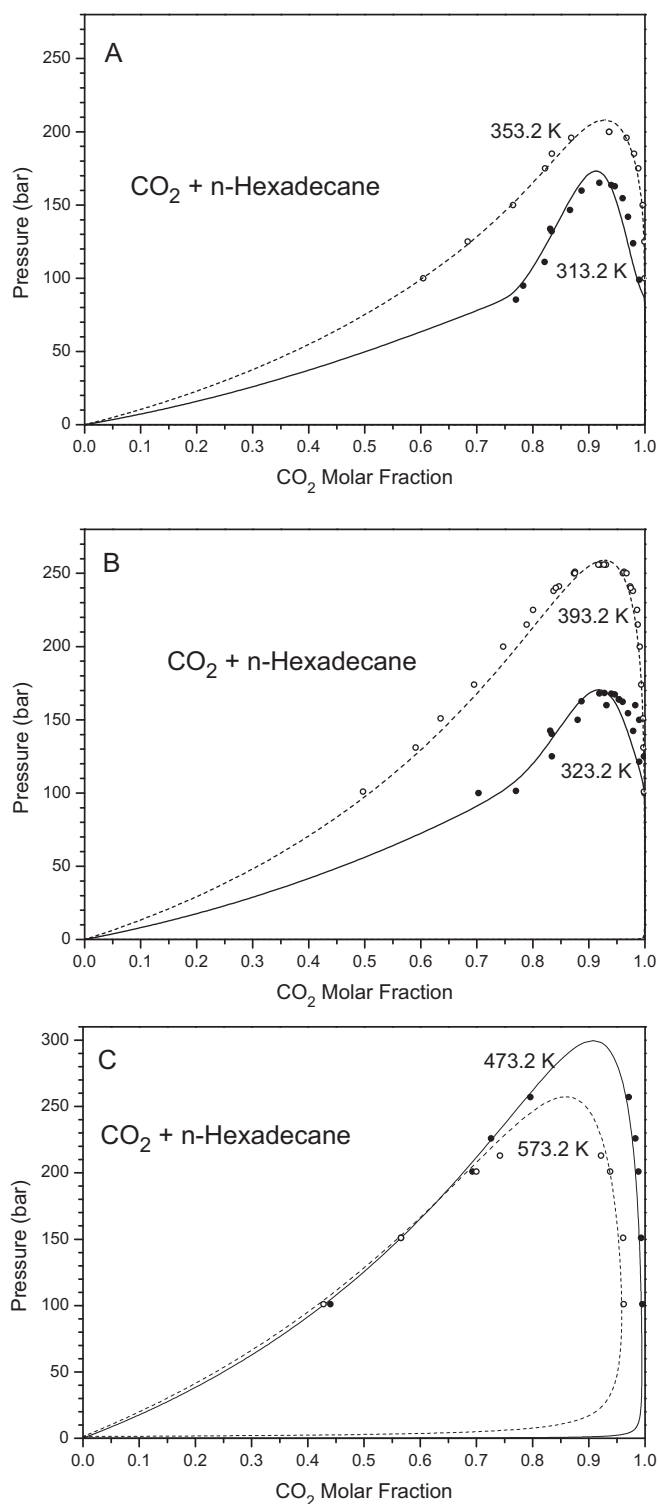


**Fig. 7.** Prediction of Pxy diagrams for the system  $\text{CO}_2$  + n-hexadecane at six different temperatures, and comparison to data from Nieuwoudt et al. [49] (313.2 and 323.2), Pöhler [42] (323.2 K), Kordikowski and Schneider [43] (353.2), Spee and Schneider [48] (393.2) and Brunner et al. [41] (473.2 and 573.2 K). Only points for two pressures at 393.2 K and two pressures at 573.2 K were considered in the parameter fitting process (see Table 4). Lines were calculated with the RK-PR EOS coupled with CMRs and parameters from Tables 1 and 5.

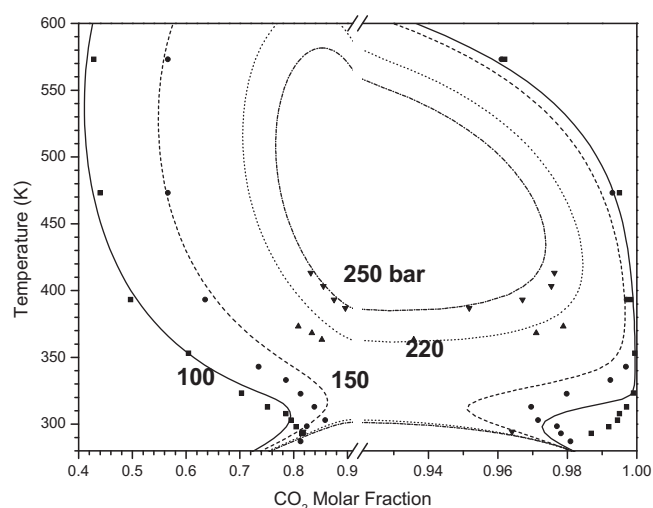


**Fig. 8.** Prediction of the Txy diagrams for the system  $\text{CO}_2$  + n-hexadecane at four different pressures, and comparison to data from Scheidgen [37] (100 and 150 bar), Brunner et al. [41] (100 and 150 bar), Pöhler [42] (220 bar) and Spee and Schneider [48] (100, 150 and 250 bar). Lines were calculated with the RK-PR EOS coupled with CMRs and parameters from Tables 1 and 5.

of temperature and pressure, have been considered for building the objective function.

On the other side, the predictions presented in Figs. 9 and 10 for the binaries with C19 and C20 seem to suffer from some systematic deviations with respect to experimental data, particularly in the heavy phase. This is clearly a consequence of not having included two phase equilibrium points besides critical line and LLV information for these systems. The result is a good matching of the critical pressure while underestimating the composition range in which phase separation occurs at lower pressures. This is a well-known behavior for analytical equation-of-state-type models not accounting for long range fluctuations in the critical region. Still, the results obtained for  $\text{CO}_2$  + n-hexadecane in Fig. 7 show that CMRs make possible to achieve a much better overall agreement, between the model and the experimental data, when both critical point and phase equilibrium information are considered. And, when looking at the behavior in a wider temperature range, like in the Txy diagram shown in Fig. 11, we see that the predictions obtained in this work are already quite acceptable for systems like

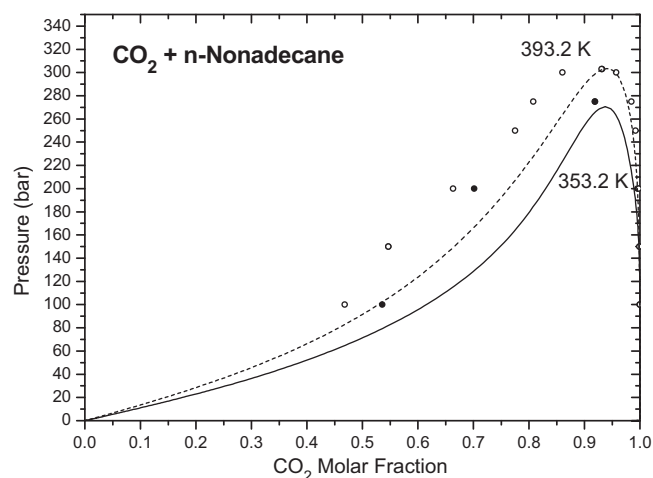


**Fig. 9.** Prediction of the Pxy diagrams for  $\text{CO}_2$  + n-nonadecane at 353.2 K (solid line) and 393.2 K (dashed line), and comparison to data from Kordikowski and Schneider [43]. Lines were calculated with the RK-PR EOS coupled with CMRs and parameters from Tables 1 and 5.



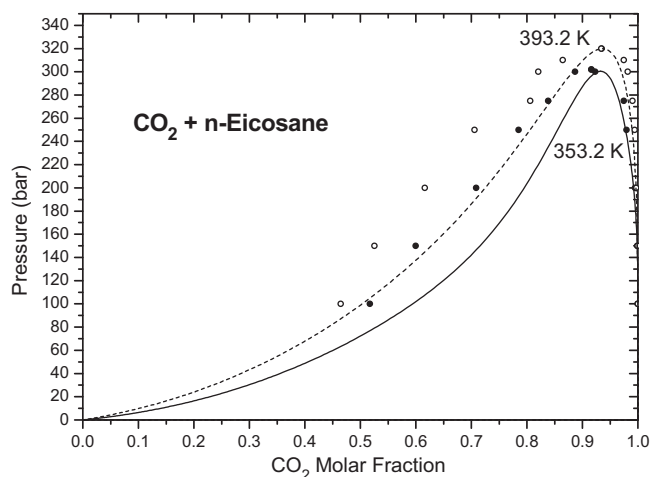


**Fig. 10.** Prediction of the Pxy diagrams for CO<sub>2</sub> + n-eicosane at 353.2 K (solid line) and 393.2 K (dashed line), and comparison to data from Kordikowski and Schneider [43]. Lines were calculated with the RK-PR EOS coupled with CMRs and parameters from Tables 1 and 5.

CO<sub>2</sub> + n-nonadecane, with parameters regressed from only a few selected critical line and LLV points.

The only clear systematic deviation that can be observed for different systems when comparing calculations to experimental data, including CO<sub>2</sub> + n-hexadecane, is in the composition of the light liquid phases along the LLV range for the cases of C14, C15 and C16 (Fig. 6). And still the magnitude of that error, which appears magnified by the scale in the figure, is not very important for the CO<sub>2</sub> mole fractions. Note that these deviations appear to be expressed with more clarity for CO<sub>2</sub> + n-tetradecane, the system which is closest to show a double critical end point (which would mark the transition to Type IV) and could therefore be related to the common limitations of analytical models in near-critical regions, which could possibly be overcome by implementing a crossover approach.

Although a deeper study of barotropic and/or isopycnic behavior is beyond the scope of the present work, we show in Fig. 12 the predicted densities for the three phases along LLV equilibrium for CO<sub>2</sub> + n-hexadecane and we also show the corresponding experimental data. The quality of the predictions both for the vapor and for the alkane-rich liquid phases is remarkable considering that no

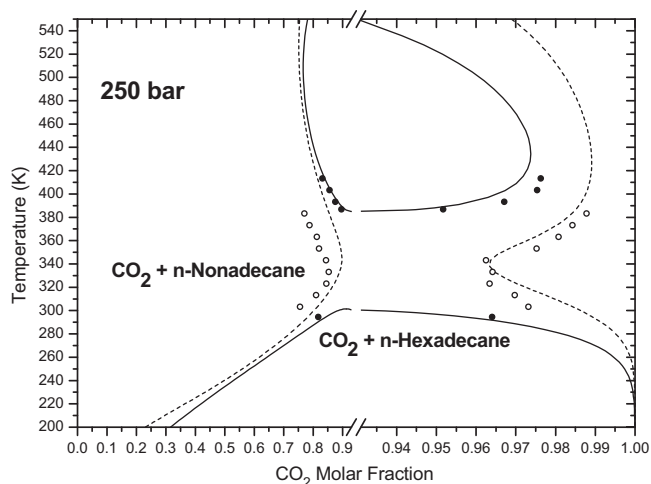


**Fig. 11.** Prediction of the Txy diagrams for CO<sub>2</sub> + n-hexadecane (solid line) and CO<sub>2</sub> + n-nonadecane (dashed line) at 250 bar, and comparison to data from Spee and Schneider [48] and Kordikowski and Schneider [43]. Lines were calculated with the RK-PR EOS coupled with CMRs and parameters from Tables 1 and 5.

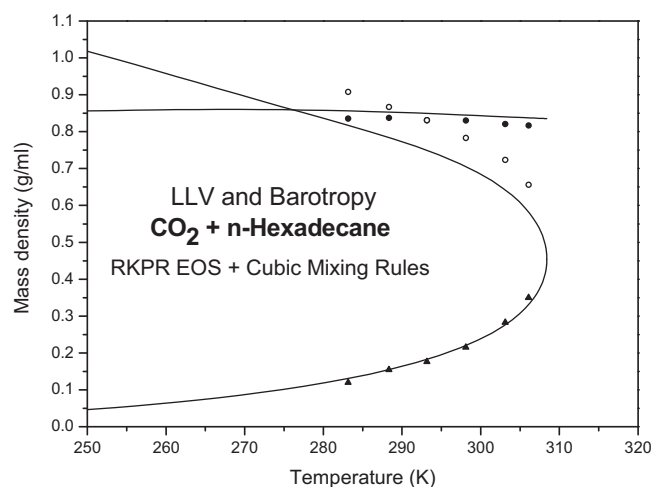


**Fig. 12.** Prediction of density and barotropy along the LLV equilibrium region for CO<sub>2</sub> + n-hexadecane, and comparison to data (markers) from van der Steen et al. [38]. Lines were calculated with the RK-PR EOS coupled with CMRs and parameters from Tables 1 and 5.

mixture density data has been considered as input for the present study. Nevertheless, there is a 10% underestimation of the CO<sub>2</sub>-richer liquid density. This could be related, at first sight, to the error in composition for the same phase, which can be observed in Fig. 6 and was referred in the previous paragraph. Actually, it is more the consequence of the underestimation of pure CO<sub>2</sub> saturated liquid densities in the temperature range considered. We expect an improvement in the description of CO<sub>2</sub>-rich liquid phases (and, consequently, also in barotropy temperatures) if the CO<sub>2</sub> parameters in Table 1 are modified in order to match the saturated liquid density, not at the triple point (216.6 K) but at a higher temperature.

In summary, we can see that the results obtained through the automated procedure for parameter fitting proposed in this work, based on a judicious definition of the objective function, led to significant improvements in the representation of phase behavior of CO<sub>2</sub> + n-alkane binary systems, both when comparing to our previous preliminary studies and to other authors approaches.

The reader might tend to believe that this good representation of phase behavior for complex binary systems could be ascribed, at first sight, only to the added mathematical flexibility obtained from the greater number of available interaction parameters for CMRs, when compared to QMRs. Nevertheless, note that, although a strictly rigorous theoretical basis for the CMRs might not be found, it is generally accepted that molecular interactions between two given types of molecules can be different, in terms of both geometrical arrangements and energetically, depending on the concentration of the mixture, especially when comparing the opposite limits of infinite dilution. And, as already pointed out in Section 1, that is exactly what the CMRs interaction parameters account for, i.e., they affect independently the properties of compound A infinitely diluted in B, and those corresponding to B infinitely diluted in A. It is also important to stress that, in this work, we have used CMRs for both, the mixture attractive parameter, and the mixture co-volume (repulsive) parameter. Thus, we have accounted for the differences existing for the opposite limits of infinite dilution not only with regard to the attractive forces but also with respect to the repulsive forces, which, as quite generally accepted, significantly affect the thermodynamic properties of dense fluids.

#### 4. Conclusions

In this work we have demonstrated that, in combination with temperature dependent attractive interaction parameters, the flex-

ibility that cubic mixing rules offer with respect to composition, in comparison to the classical quadratic mixing rules, can be used to accurately represent the phase equilibria of highly asymmetric binary mixtures showing type III phase behavior, like CO<sub>2</sub> + n-alkanes, and in the full ranges of temperature and pressure available.

In our study the objective function for the optimization of parameters used four critical line key-points and six LLV key-points for each system. In addition, it also included a few carefully selected two-phase points only for CO<sub>2</sub> + n-hexadecane, the system with more complete experimental information available. From the results we draw the following conclusions for CO<sub>2</sub> + n-alkanes binary mixtures showing type III phase behavior (C14 to C22):

- (1) The cubic mixing rules (CMRs), used for both, the attractive and the repulsive mixture parameters, together with temperature-dependent interaction parameters, coupled to the RK-PR EoS, made it possible to achieve the best simultaneous representation of critical lines and LLV equilibria that, to our knowledge, has ever been reported, irrespective to the modeling approach used, in the open literature.
- (2) Equivalent accuracy is not guaranteed for predictions of liquid–vapor equilibrium, specially at higher temperatures, if no representative points are considered for the optimization.
- (3) A correct and accurate overall description of the phase behavior is possible through a proper balance in the objective function, that combines critical line and LLV information with representative two-phase data points, as it was done for CO<sub>2</sub> + n-hexadecane in this work.

From these conclusions and from the experience we gained in the present study, a predictive correlation will be developed in a new work, which we expect will provide complete results for the whole series as good as those presented for CO<sub>2</sub> + n-hexadecane in this work.

## Acknowledgments

We are grateful to Prof. Esteban A. Brignole of Planta Piloto de Ingeniería Química (Universidad Nacional del Sur-CONICET), for bringing the problem on which we focus in this work to our attention, and for helpful comments and discussions. We also thank Prof. Schneider (University of Bochum, Germany) for kindly providing us with copies of master and Ph.D. thesis of his group, containing valuable unpublished data. Finally, we acknowledge the financial support received from the following institutions: Consejo Nacional de Investigaciones Científicas y Técnicas de la República Argentina, Agencia Nacional de Promoción Científica y Tecnológica de la República Argentina, Universidad Nacional del Sur, Universidad Nacional de Córdoba and IVC-SEP (DTU, Denmark).

## References

- [1] J.D. van der waals, Over de continuïteit van den gas-en vloeistoestand, Leiden University, 1873.
- [2] J.M.H. Levelt Sengers, Gas–gas equilibria—from Van der Waals to Ulrich Franck, *J. Supercritical Fluids* 39 (2006) 144–153.
- [3] J. de Swaan Arons, W.Th. de Loos, Phase behavior: phenomena, significance, and models, in: S.I. Sandler (Ed.), *Models for Thermodynamic and Phase Equilibria Calculations*, Marcel-Dekker, New York, 1993, p. 442.
- [4] J.M. Milanese, M. Cismondi, L. Cardozo-Filho, L.M. Quinzani, M.S. Zabaloy, Phase behavior of linear mixtures in the context of equation of state models, *Industrial and Engineering Chemistry Research* 49 (2010) 2943–2956.
- [5] C. Tsionopoulos, J.L. Heidman, High-pressure vapor–liquid equilibria with cubic equations of state, *Fluid Phase Equilibria* 29 (1986) 391–414.
- [6] E.C. Voutsas, G.D. Pappa, K. Magoulas, D.P. Tassios, Vapor liquid equilibrium modeling of alkane systems with equations of state: “simplicity versus complexity”, *Fluid Phase Equilibria* 240 (2006) 127–139.
- [7] J.O. Valderrama, The state of the cubic equations of state, *Industrial and Engineering Chemistry Research* 42 (2003) 1603–1618.

- [8] I. Polishuk, J. Wisniak, H. Segura, Simultaneous prediction of the critical and sub-critical phase behavior in mixtures using equations of state II. Carbon dioxide-heavy n-alkanes, *Chemical Engineering Science* 58 (2003) 2529–2550.
- [9] M. Cismondi, J. Mollerup, Development and application of a three-parameter RK-PR equation of state, *Fluid Phase Equilibria* 232 (2005) 74–89.
- [10] M. Cismondi, *Ingeniería Del Equilibrio Entre Fases: Diagramas Globales Y Modelo De Mezclas Asimétricas Con CO<sub>2</sub>*, Universidad Nacional del Sur, Bahía Blanca, Argentina, 2006.
- [11] S. Vitu, R. Privat, J.N. Jaubert, F. Mutelet, Predicting the phase equilibria of CO<sub>2</sub> + hydrocarbon systems with the PPR78 model (PR EOS and kij calculated through a group contribution method), *J. Supercritical Fluids* 45 (2008) 1–26.
- [12] D.B. Robinson, D.Y. Peng, *The Characterization of the Heptanes and Heavier Fractions for the GPA Peng–Robinson Programs*, Gas Processors Association, 1978.
- [13] D.J. Fall, K.D. Luks, Liquid–liquid–vapor phase equilibria of the binary system carbon dioxide + n-tridecane, *J. Chemical and Engineering Data* 30 (1985) 276–279.
- [14] D. Fu, L. Liang, X.S. Li, S. Yan, T. Liao, Investigation of vapor–liquid equilibria for supercritical carbon dioxide and hydrocarbon mixtures by perturbed-chain statistical associating fluid theory, *Industrial and Engineering Chemistry Research* 45 (2006) 4364–4370.
- [15] D. Nguyen-Huynh, J.P. Passarello, P. Tobaly, J.C. De Hemptinne, Modeling phase equilibria of asymmetric mixtures using a group-contribution SAFT (GC-SAFT) with a kij correlation method based on London's theory. 1. Application to CO<sub>2</sub> + n-Alkane, methane + n-alkane, and ethane + n-alkane systems, *Industrial and Engineering Chemistry Research* 47 (2008) 8847–8858.
- [16] A. Haghtalab, P. Mahmoodi, Vapor–liquid equilibria of asymmetrical systems using UNIFAC-NRF group contribution activity coefficient model, *Fluid Phase Equilibria* 289 (2010) 61–71.
- [17] C. Kun, C. Zhen-hua, Y. Zhen, L. Yan, H. Zhi-ming, Prediction of vapor–liquid equilibrium at high pressure using a new excess free energy mixing rule coupled with the original UNIFAC method and the SRK equation of state, *Industrial and Engineering Chemistry Research* 48 (2009) 6836–6845.
- [18] X. Tang, J. Gross, Modeling the phase equilibria of hydrogen sulfide and carbon dioxide in mixture with hydrocarbons and water using the PC-SAFT equation of state, *Fluid Phase Equilibria* 293 (2010) 11–21.
- [19] M.S. Zabaloy, Cubic mixing rules, *Industrial and Engineering Chemistry Research* 47 (2008) 5063–5079.
- [20] I. Polishuk, An empirical modification of classical mixing rule for the cohesive parameter: the triple interactions in binary systems considered, *Industrial & Engineering Chemistry Research* 49 (2010) 4989–4994.
- [21] G. Pisoni, M. Cismondi, M.S. Zabaloy, The influence of ternary interaction parameters on the representation of the high-pressure fluid phase equilibria of ternary systems, in: C.G. Pereira, O. Chiavone-Filho (Eds.), *II Iberoamerican Conference on Supercritical Fluids (PROSCIBA 2010)*, Natal, Brazil, 2010.
- [22] M. Cismondi, J. Mollerup, M.S. Zabaloy, Performance of cubic mixing rules on the description of high pressure fluid phase equilibria, in: *1st Iberoamerican Conference on Supercritical Fluids PROSCIBA 2007*, Foz do Iguaçu, Brazil, 2007.
- [23] M. Cismondi, J.M. Mollerup, M.S. Zabaloy, Modeling the fluid phase equilibria of asymmetric CO<sub>2</sub>–hydrocarbon systems using a consistent cubic composition dependency, in: J.-N. Jaubert (Ed.), *23rd ESAT, European Symposium on Applied Thermodynamics*, Cannes, France, 2008.
- [24] R.L. Scott, P.H. Van Konynenburg, Static properties of solutions: Van der Waals and related models for hydrocarbon mixtures, *Discussions of the Faraday Society* 49 (1970) 87–97.
- [25] M. Cismondi, D.N. Nuñez, M.S. Zabaloy, E.A. Brignole, M.L. Michelsen, J.M. Mollerup, GPEC: a program for global phase equilibrium calculations in binary systems, in: *EQUIFASE 2006: VII Iberoamerican Conference on Phase Equilibria and Fluid Properties for Process Design*, Morelia, Michoacán, México, 2006.
- [26] M. Cismondi, D.N. Nuñez, in: M.S. Zabaloy, E.A. Brignole (Eds.), *GPEC (Global Phase Equilibrium Calculations)*, Bahía Blanca and Córdoba, 2005–2009, [www.gpec.efn.uncor.edu](http://www.gpec.efn.uncor.edu).
- [27] R. Privat, R. Gani, J.N. Jaubert, Are safe results obtained when the PC-SAFT equation of state is applied to ordinary pure chemicals? *Fluid Phase Equilibria* 295 (2010) 76–92.
- [28] M.F. Alfradique, M. Castier, Calculation of phase equilibrium of natural gases with the Peng–Robinson and PC-SAFT equations of state, *Oil and Gas Science and Technology* 62 (2007) 707–714.
- [29] S.A. Martinez, K.R. Hall, Thermodynamic properties of light synthetic natural gas mixtures using the RK-PR cubic equation of state, *Industrial and Engineering Chemistry Research* 45 (2006) 3684–3692.
- [30] A.R.J. Arendsen, G.F. Versteeg, Dynamic thermodynamics with internal energy, volume, and amount of moles as states: application to liquefied gas tank, *Industrial and Engineering Chemistry Research* 48 (2009) 3167–3176.
- [31] R.L. Rowley, W.V. Wilding, J.L. Oscarson, Y. Yang, N.A. Zundel, T.E. Daubert, R.P. Danner, *DIPPR Data Compilation of Pure Compound Properties*, Design Institute for Physical Properties, AIChE, New York, 2003.
- [32] I. Polishuk, J. Wisniak, H. Segura, Simultaneous prediction of the critical and sub-critical phase behavior in mixtures using equation of state I. Carbon dioxide-alkanols, *Chemical Engineering Science* 56 (2001) 6485–6510.
- [33] C. Secuianu, V. Ferioiu, D. Geană, Phase behavior for carbon dioxide + ethanol system: experimental measurements and modeling with a cubic equation of state, *J. Supercritical Fluids* 47 (2008) 109–116.
- [34] C. Secuianu, V. Ferioiu, D. Geană, High-pressure phase equilibria for the carbon dioxide + 1-propanol system, *J. Chemical & Engineering Data* 53 (2008) 2444–2448.

- [35] C. Secuianu, V. Ferioli, D. Geană, Phase behavior for the carbon dioxide + 2-butanol system: experimental measurements and modeling with cubic equations of state, *J. Chemical & Engineering Data* 54 (2009) 1493–1499.
- [36] A. Scheidgen, Fluidphasengleichgewichte von CO<sub>2</sub> + 1-Nonanol + Pentadecan und CO<sub>2</sub> + 1-Nonanol + Hexadecan bis 100 MPa. Cosolvency effect und Miscibility windows, Ruhr-Universität Bochum, Bochum, 1994.
- [37] A. Scheidgen, Fluidphasengleichgewichte binärer und ternärer Kohlendioxidmischungen mit schwerflüchtigen organischen Substanzen bis 100 MPa. Cosolvency Effect, Miscibility windows und Löcher in der kritischen Fläche, Ruhr-Universität Bochum, Bochum, 1997.
- [38] J. van der Steen, T.W. de Loos, J. de Swaan Arons, The volumetric analysis and prediction of liquid–liquid–vapor equilibria in certain carbon dioxide + n-alkane systems, *Fluid Phase Equilibria* 51 (1989) 353–367.
- [39] J.D. Hottovy, K.D. Luks, J.P. Kohn, Three-phase liquid–liquid–vapor equilibrium behavior of certain binary CO<sub>2</sub>-n-paraffin systems, *J. Chemical and Engineering Data* 26 (1981) 256–258.
- [40] D.J. Fall, J.L. Fall, K.D. Luks, Liquid–liquid–vapor immiscibility limits in carbon dioxide + n-paraffin mixtures, *J. Chemical and Engineering Data* 30 (1985) 82–88.
- [41] G. Brunner, J. Teich, R. Dohrn, Phase equilibria in systems containing hydrogen, carbon dioxide, water and hydrocarbons, *Fluid Phase Equilibria* 100 (1994) 253–268.
- [42] H. Pohler, Fluidphasengleichgewichte Binärer und Ternärer Kohlendioxidmischungen mit Schwerflüchtigen Organischen Substanzen bei Temperaturen von 303 K bis 393 K und Drücken von 10 MPa bis 100 MPa, Ruhr-Universität Bochum, Bochum, 1994.
- [43] A. Kordikowski, G.M. Schneider, Fluid phase equilibria of binary and ternary mixtures of supercritical carbon dioxide with low-volatility organic substances up to 100 MPa and 393 K, *Fluid Phase Equilibria* 90 (1993) 149–162.
- [44] M. Cismondi, M. Michelsen, Automated calculation of complete Pxy and Txy diagrams for binary systems, *Fluid Phase Equilibria* 259 (2007) 228–234.
- [45] M. Cismondi, M.L. Michelsen, Global phase equilibrium calculations: critical lines, critical end points and liquid–liquid–vapour equilibrium in binary mixtures, *J. Supercritical Fluids* 39 (2007) 287–295.
- [46] M. Cismondi, M.L. Michelsen, M.S. Zabaloy, Automated generation of phase diagrams for binary systems with azeotropic behavior, *Industrial and Engineering Chemistry Research* 47 (2008) 9728–9743.
- [47] A.L. Scheidgen, G.M. Schneider, Complex phase equilibrium phenomena in fluid ternary mixtures up to 100 MPa: cosolvency, holes, windows, and islands—review and new results, *Fluid Phase Equilibria* 194–197 (2002) 1009–1028.
- [48] M. Spee, G.M. Schneider, Fluid phase equilibrium studies on binary and ternary mixtures of carbon dioxide with hexadecane, 1-dodecanol, 1,8-octanediol and dotriacontane at 393.2 K and at pressures up to 100 MPa, *Fluid Phase Equilibria* 65 (1991) 263–274.
- [49] I. Nieuwoudt, M. Du Rand, Measurement of phase equilibria of supercritical carbon dioxide and paraffins, *J. Supercritical Fluids* 22 (2002) 185–199.